BIOORGANIC CHEMISTRY **25,** 130–153 (1997)
ARTICLE NO. BH971061

Further Insights into the Oxidation Chemistry of Norepinephrine and Epinephrine in the Presence of Cysteine

Xue-Ming Shen and Glenn Dryhurst[1]

Department of Chemistry and Biochemistry, University of Oklahoma, Norman, Oklahoma 73019

Received March 12, 1997

Oxidations of dopamine (DA), norepinephrine (NE), and epinephrine (EPI) at pH 7.4 in the presence of free L-cysteine (CySH) have been previously shown to generate a number of cysteinyl conjugates of these catecholaminergic neurotransmitters that serve as precursors of various dihydrobenzothiazines (DHBTs). In this investigation it is demonstrated that oxidations of NE or EPI, but not DA, in the presence of free CySH also generate three previously unknown DHBTs: 6,8-bis[(2-amino-2-carboxyethyl)thio]-3,4-dihydro-5-hydroxy-2*H*-1,4-benzothiazine-3-carboxylic acid (**A**), 6,7,8-tris[(2-amino-2-carboxyethyl)thio]-3,4-dihydro-5-hydroxy-2*H*-1,4-benzothiazine-3-carboxylic acid (**B**), and *N*-[9-[(2-amino-2-carboxyethyl)thio]-7-carboxy-3,6,7,8-tetrahydro-10-hydroxybenzo[1,2-*b*: 4,3-b′]bis[1,4]thiazin-2-yl]-L-cystine (**C**). The *β*-hydroxy side chain residues of NE and EPI are required in order to form **A–C,** hence explaining the fact that these compounds are not formed upon oxidation of DA in the presence of CySH. A further new product unique to the oxidation of EPI in the presence of CySH at pH 7.4 is *N*-[6-[(2-amino-2-carboxyethyl)thio]-2,7-dihydro-5-hydroxy-7-methylpyrrolo[2,3-*h*]-1,4-benzothiazin-3-yl]-L-cystine (**D**). Reactions pathways that account for formation of **A–D** are presented along with a discussion of their potential formation as aberrant metabolites in the brain in a number of neurodegenerative disorders.

INTRODUCTION

Recent reports from this laboratory have described the first detailed studies into the influence of L-cysteine (CySH) on the *in vitro* oxidation chemistry of the catecholaminergic neurotransmitters dopamine (DA) (*1–4*), norepinephrine (NE) (*5*), and epinephrine (EPI) (*6*) at pH 7.4. Our interest in such studies stem from the hypothesis that such chemistry might occur within catecholaminergic neurons in a number of neurodegenerative brain disorders and that the resulting products (metabolites) might include endotoxins that contribute to the pathological mechanisms underlying these disorders (*1–6*).

The chemical, enzyme-mediated, and electrochemically driven oxidations of DA, NE, and EPI generate *o*-quinone proximate products (*7–14*). In the absence of CySH or glutathione (GSH) at pH 7.4, deprotonation of the exocyclic amino group yields the neutral *o*-quinones that undergo an intramolecular cyclization reaction

[1] To whom correspondence should be addressed. Fax: (405) 325-6111. E-mail: gdryhurst@chemdept.chem.uoknor.edu.

0045-2068/97 $25.00

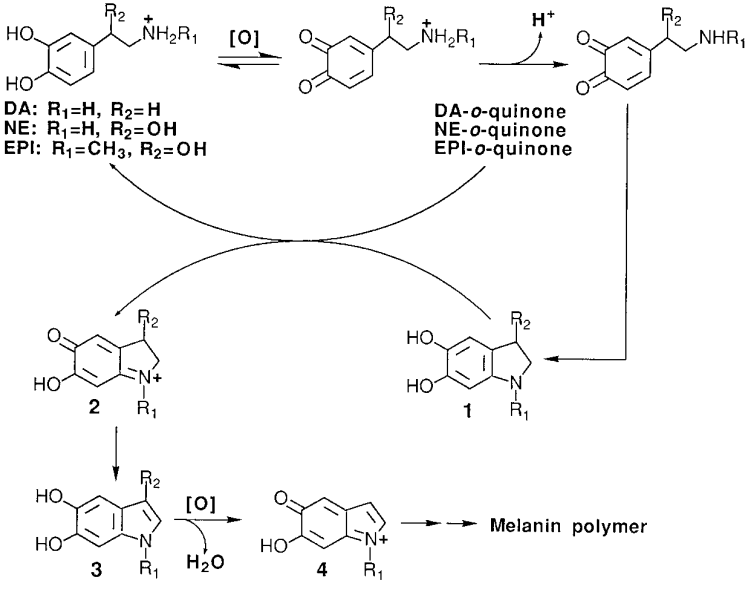

SCHEME 1

to give 5,6-dihydroxyindolines (**1,** Scheme 1). The latter compounds are then oxidized by the catecholamine-*o*-quinone precursor to the aminochromes **2** (*9*, *10*, *12*) that rearrange to the corresponding 5,6-dihydroxyindole (**3**). Further oxidation (2*e*) of **3** (and loss of the elements of water from the compounds formed from NE and EPI) generates the *p*-quinone imine **4** that reacts with various precursor species in a poorly understood pathway, leading ultimately to dark, insoluble melanin polymer. Using electrochemical techniques to oxidize DA (*1–4*), NE (*5*), and EPI (*6*) at pH 7.4, it has been found that CySH diverts or, at sufficiently high concentrations, blocks formation of melanin polymer by scavenging the *o*-quinone proximate oxidation products to form, initially, the 5-*S*-cysteinyl (major route) and 2-*S*-cysteinyl conjugates of these neurotransmitters (Scheme 2). These cysteinyl conjugates are appreciably more easily oxidized than their parent catecholamines to give *o*-quinones **5** and **6,** respectively. Nucleophilic addition of CySH to **5** and **6** then yields the 2,5-bis-*S*-cysteinyl conjugates of DA, NE, and EPI that, by a similar reaction sequence, give the corresponding 2,5,6-tris-*S*-cysteinyl catecholamines. However, *o*-quinones **5** can also undergo intramolecular cyclization to *o*-quinone imines **7** that can chemically oxidize the parent 5-*S*-cysteinylcatecholamine (5-*S*-CyS-CA) to give **5** and radical **8** (Scheme 2). Radicals **8** then disproportionate (*15*) to *o*-quinone imines **7** and the dihydrobenzothiazines (DHBTs) DHBT-1, DHBT-NE-1, or DHBT-EPI-1 (*1–6*).[2] A similar reaction pathway leads to DHBT-5, DHBT-NE-5, and DHBT-EPI-5 by oxidations of the 2-*S*-cysteinyl conjugates of DA, NE, and EPI respectively,

[2] Abbreviations are the same as employed in earlier papers (*1–6*).

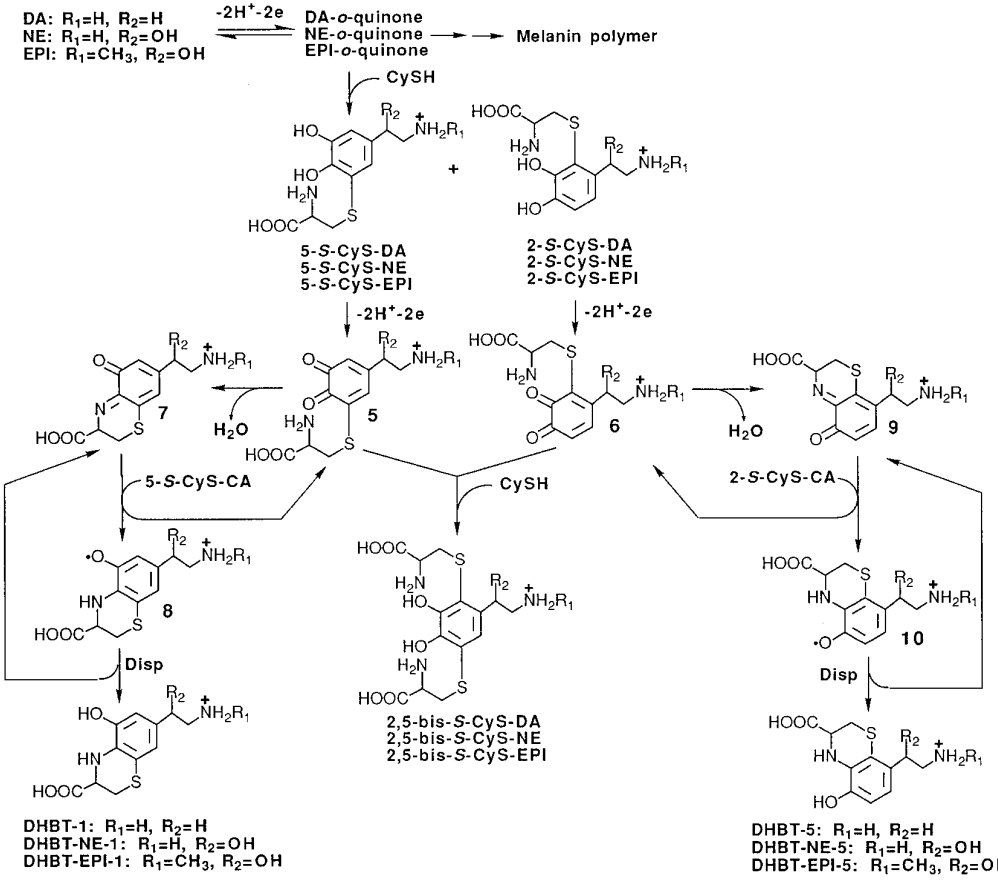

SCHEME 2

as shown in Scheme 2. Oxidations of more highly substituted cysteinyl conjugates of these catecholamines, and nucleophilic additions of CySH to cyclic *o*-quinone imines such as **7** and **9,** provide routes to even more structurally complex DHBTs. The cysteinyl conjugates and resultant DHBTs formed by the electrochemically driven oxidations of the catecholamine neurotransmitters in the presence of CySH reported previously all retain the ethylamino side chain residue of DA, NE, or EPI. However, in continuing studies aimed at more completely elucidating the products of these reactions, i.e., putative *in vivo* metabolites, it was noted that oxidations of NE and EPI, but not DA, in the presence of relatively large excesses of CySH gave rise to a number of other previously unreported products. These products were unusual because their chromatographic and spectroscopic properties suggested that they were the same whether the oxidized catecholamine was NE or EPI. This in turn suggested that these products might be formed in an unusual reaction in which the β-hydroxyethylamino side chain residues of NE and EPI are eliminated.

Several DHBTs formed as a result of the oxidation of the catecholaminergic

neurotransmitters in the presence of CySH are toxic (lethal) when administered into the brains of mice (*1–5*). This observation lends some support to the hypothesis that these putative metabolites might be endotoxins involved in the overall pathogenesis of certain neurodegenerative brain disorders. It was clearly of interest, therefore, to isolate and identify the new products apparently common to the oxidations of NE and EPI in the presence of CySH. This communication, therefore, describes conditions under which these putative metabolites can be formed and chromatographically isolated and purified. Spectroscopic evidence in support of the proposed structures of these novel compounds is also provided.

EXPERIMENTAL

(−)-Norepinephrine hydrochloride (NE·HCl), (−)-epinephrine (EPI), dopamine hydrochloride (DA·HCl), and L-cysteine (CySH) were obtained from Sigma (St. Louis, MO). Tris(2-carboxyethyl)phosphine hydrochloride (TCEP·HCl) was obtained from Pierce (Rockford, IL). Trifluoroacetic acid (TFA) was obtained from Aldrich (Milwaukee, WI) and HPLC grade acetonitrile (MeCN) from EM Science (Gibbstown, NJ).

7-(1-Hydroxy-2-aminoethyl)-3,4-dihydro-5-hydroxy-2*H*-1,4-benzothiazine-3-carboxylic acid (DHBT-NE-1) and its 6-*S*-cysteinyl conjugate (DHBT-NE-2), 8-(1-hydroxy-2-aminoethyl)-3,4-dihydro-5-hydroxy-2*H*-1,4-benzothiazine-3-carboxylic acid (DHBT-NE-5), its 6-*S*-cysteinyl conjugate (DHBT-NE-6), and 6,7-bis-*S*-cysteinyl conjugate (DHBT-NE-7) were synthesized as described previously (*5*). Syntheses of 5-*S*-cysteinylepinephrine (5-*S*-CyS-EPI), 2-*S*-CyS-EPI, 2,5-bis-*S*-CyS-EPI, 7-[(2-methylamino)ethyl]-3,4-dihydro-5-hydroxy-2*H*-1,4-benzothiazine-3-carboxylic acid (DHBT-EPI-1), its 6-*S*-cysteinyl conjugate (DHBT-EPI-2), 8-[(2-methylamino)ethyl]-3,4-dihydro-5-hydroxy-2*H*-1,4-benzothiazine-3-carboxylic acid (DHBT-EPI-5), its 6-*S*-cysteinyl conjugate (DHBT-EPI-6), and 6,7-bis-*S*-cysteinyl conjugate (DHBT-EPI-7) have been reported earlier (*6*).

Voltammograms were obtained at a pyrolytic graphite electrode (PGE; Pfizer Minerals, Pigments and Metals Division, Easton, PA) having an approximate surface area of 6 mm^2. A conventional three-electrode voltammetric cell was used with a platinum wire counter electrode and a saturated calomel reference electrode (SCE). Cyclic voltammograms were obtained with a BAS 100A (Bioanalytical Systems, West Lafeyette, IN) electrochemical analyzer. The PGE was resurfaced prior to recording each voltammogram; all voltammograms were corrected for ir drop. Controlled potential electrolyses employed a Princeton Applied Research Corporation (Princeton, NJ) Model 173 potentiostat and a three-compartment cell in which the working, counter, and reference electrodes were separated with a Nafion membrane (type 117, DuPont Co., Wilmington, DE). The working electrode consisted of several plates of pyrolytic graphite having an approximate surface area of 180 cm^2. The counter electrode was platinum gauze and the reference electrode a SCE. The solution in the working electrode compartment was continuously bubbled with a vigorous stream of N_2 and stirred with a Teflon-coated magnetic stirring bar. All potentials are referenced to the SCE at ambient temperature (22 ± 2°C).

NMR spectra (^{1}H and ^{13}C) were recorded on either a Varian (Palo Alto, CA) XL-300 or a Varian VXR-500 spectrometer. Fast atom bombardment mass spectra (FAB-MS) were obtained with a VG Instruments (Manchester, UK) Model ZAB-E spectrometer. UV–visible spectra were recorded on a Hewlett-Packard (Palo Alto, CA) Model 8452A diode array spectrometer.

Preparative high performance liquid chromatography (HPLC) was carried out with a Gilson (Middleton, WI) gradient system equipped with dual Model 302 pumps (10 ml pump heads), a Rheodyne (Cotati, CA) Model 7125 loop injector, and a Waters (Milford, MA) Model 440 uv detector set at 254 nm. A reversed phase column (Bakerbond C_{18}, 10 μm, 250 $\times$ 21.2-mm; P. J. Cobert Associates, St. Louis, MO) and two mobile phase solvents were employed. Solvent A was prepared by adding concentrated TFA to deionized water until the pH was 2.15. Solvent B was prepared by adding TFA to a 1:1 solution (v/v) of deionized water and MeCN until the pH was 2.15. HPLC method I employed the following mobile phase gradient: 0–5 min, 100% solvent A; 5–40 min, linear gradient to 12% solvent B; 40–80 min, linear gradient to 50% solvent B; 80–85 min, linear gradient to 100% solvent B; 85–97 min, 100% solvent B. HPLC method II: 0–85 min, linear gradient from 100% solvent A to 15% solvent B; 85–130 min, linear gradient to 45% solvent B; 130–134 min, linear gradient to 100% solvent B; 134–146 min, 100% solvent B. HPLC Method III: 0–20 min, 100% solvent A; 20–140 min, linear gradient to 26% solvent B; 140–144 min, linear gradient to 100% solvent B; 144–156 min, 100% solvent B. HPLC Method IV: 0–2 min; 100% solvent A; 2–80 min, linear gradient to 60% solvent B; 80–90 min, linear gradient to 100% solvent B; 90–102 min, 100% solvent B. The flow rate for HPLC methods I–IV was 7 ml min^{-1}.

Oxidation Reaction Procedures

NE·HCl (3.1 mg; 0.5 mM), or EPI (2.75 mg; 0.5 mM), or DA·HCl (2.85 mg; 0.5 mM) and CySH (9.1 mg; 2.5 mM) were dissolved in 30 ml of pH 7.4 phosphate buffer (μ = 0.2) and the resulting solution was electrolyzed at 70 mV for 30 min. Upon termination of the reaction the entire yellow solution was pumped onto the reversed phase column and products separated using HPLC method I(NE), II (EPI), or III (DA). The solutions eluted under the chromatographic peaks corresponding to each product were collected individually, immediately frozen at -80°C (dry ice), and then freeze–dried. The resulting products were then dissolved in the minimum volume of deionized water and purified by the appropriate HPLC method at least one more time. The purity of each product was further determined by analytical HPLC with electrochemical detection (HPLC-EC). HPLC-EC employed a BAS PM-80 pump, a Rheodyne 7125 injector with a 5.0-μL sample loop, and a BAS LC-4C electrochemical detector equipped with a glassy carbon detector electrode set at 800 mV vs Ag/AgCl reference electrode. A reversed phase column (BAS, Phase-II ODS, 3 μm, 100 $\times$ 3.2 mm) was employed. The mobile phase consisted of 0.085% diethylamine (v/v), 0.05 mM Na_2 EDTA, 0.30 mM sodium octyl sulfate, and 0.1 M citric acid in 9.0% MeCN/deionized water at pH 2.31. The flow rate was constant at 0.6 ml min^{-1}.

TABLE 1

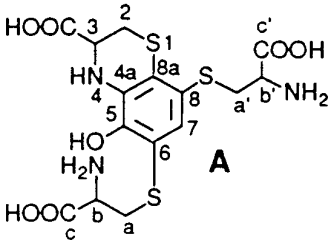

Assignment	^{1}H (J in Hz)	^{13}C	HMQC (^{13}C)	HMBC (^{13}C)
7	7.09 (s, 1H)	130.72	130.72	144.92 (5), 122.52 (8a)
3	4.53 (dd, 4.5, 3.5, 1H)	51.70	51.70	174.77 (c″), 130.85 (4a)
b′	3.98 (t, 5.5, 1H)	52.09	52.09	170.55 (c′), 34.76 (a′)
b	3.96 (dd, 7.5, 4.0, 1H)	52.17	52.17	170.46 (c), 34.95 (a)
a	3.32 (dd, 15.5, 7.5, 1H)	34.95	34.95	119.23 (6), 52.17 (b)
2	3.30 (dd, 13.5, 4.5, 1H)	26.30	26.30	122.52 (8a)
a	3.27 (dd, 15.5, 4.0, 1H)	34.95	34.95	170.46 (c), 119.23 (6), 52.17 (b)
a′	3.26 (d, 5.5, 2H)	34.76	34.76	170.55 (c′), 113.34 (8), 52.09 (b′)
2	3.15 (dd, 13.5, 3.5, 1H)	26.30	26.30	174.77 (c″), 51.70 (3)
4a		130.85		
5		144.92		
6		119.23		
8		113.34		
8a		122.52		
c		170.46		
c′		170.55		
c″		174.77		

Spectroscopic evidence in support of the proposed structures of products is presented below and, along with additional chemical evidence, is discussed further under Results. All ^{1}H NMR assignments were based at least on homonuclear decoupling and two-dimensional (2D) correlated spectrospray (COSY) experiments. However, for most compounds ^{1}H (500 MHz), ^{13}C (125 MHz), heteronuclear multiple-quantum coherence (HMQC), and heteronuclear multiple-bond connectivity (HMBC) spectra were also recorded.

6,8-Bis[(*2-amino-2-carboxyethyl*)*thio*]*-3,4-dihydro-5-hydroxy-2H-1,4-benzothiazine-3-carboxylic Acid* (**A**)

Compound **A** was a very pale yellow solid that, when dissolved in the HPLC mobile phase (pH 2.15) exhibited uv bands at λ_{max} = 326 and 256 nm. FAB-MS (glycerol/TFA matrix) gave m/e = 450.0471 (MH^+, 85%, $C_{15}H_{20}N_3O_7S_3$; Calcd. m/e = 450.0463). The ^{1}H NMR (500 MHz), ^{13}C (125 MHz), HMQC and HMBC NMR spectra (D_2O) along with the proposed structure of **A** and assignments of long-range ^{1}H–^{13}C connectivities from HMBC data are presented in Table 1.

TABLE 2

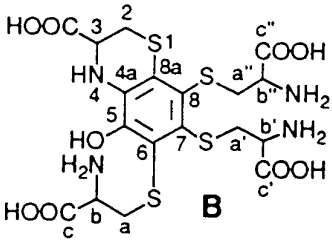

Assignment	^{1}H (J in Hz)	^{13}C	HMQC (^{13}C)	HMBC (^{13}C)
3	4.64 (t, 3.5, 1H)	51.72	51.72	174.77 (c‴), 132.63 (4a)
b	4.08 (t, 5.5, 1H)	51.59	51.59	169.86 (c), 37.44 (a)
b′	3.97 (t, 5.5, 1H)	52.06	52.06	170.28 (c′), 35.72 (a′)
b″	3.96 (dd, 7.0, 5.0, 1H)	51.97	51.97	170.37 (c″), 36.49 (a″)
a	3.53 (dd, 15.0, 5.5, 1H)	37.44	37.44	169.86 (c), 129.07 (6), 51.59 (b)
a″	3.48 (dd, 15.0, 7.0, 1H)	36.49	36.49	170.37 (c″), 126.84 (8), 51.97 (b″)
a′	3.47 (dd, 15.0, 5.5, 1H)	35.72	35.72	170.28 (c′), 119.36 (7), 52.06 (b′)
2	3.35 (dd, 13.5, 3.5, 1H)	26.79	26.79	124.11 (8a), 51.72 (3)
a	3.34 (dd, 15.0, 5.5, 1H)	37.44	37.44	169.86 (c), 129.07 (6), 51.59 (b)
a″	3.33 (dd, 15.0, 5.0, 1H)	36.49	36.49	170.37 (c″), 126.84 (8), 51.97 (b″)
a′	3.29 (dd, 15.0, 5.5, 1H)	35.72	35.72	170.28 (c′), 119.36 (7), 52.06 (b′)
2	3.12 (dd, 13.5, 3.5, 1H)	26.79	26.79	174.77 (c‴), 51.72 (3)
4a		132.63		
5		146.30		
6		129.07		
7		119.36		
8		126.84		
8a		124.11		
c		169.86		
c′		170.28		
c″		170.37		
c‴		174.77		

6,7,8-Tris[*(2-amino-2-carboxyethyl)thio*]*-3,4-dihydro-5-hydroxy-2H-1,4-benzothiazine-3-carboxylic Acid* (**B**)

Compound **B** was a very pale yellow solid that, dissolved in the HPLC mobile phase (pH 2.15), exhibited UV bands at λ_{max} = 314 and 266 nm. FAB-MS (glycerol/TFA matrix) gave m/e = 569.0509) (MH^+, 21%, $C_{18}H_{25}N_4O_9S_4$; Calcd. m/e = 569.0504). A summary of the ^{1}H (500 MHz), ^{13}C (125 MHz), HMQC, and HMBC NMR spectra (D_2O) of **B** along with its proposed structure and assignments of long range ^{1}H–^{13}C connectivities from HMBC data are presented in Table 2.

N-[*9-*[*(2-Amino-2-carboxyethyl)thio*]*-7-carboxy-3,6,7,8-tetrahydro-10-hydroxybenzo*[*1,2-b: 4,3-b′*]*bis*[*1,4*]*thiazin-2-yl*]-L-*cystine* (**C**)

Compound **C** was a yellow solid that, when dissolved in the HPLC mobile phase (pH 2.15), exhibited uv bands at λ_{max} = 372, 298 (sh), 258, and 230 nm. FAB-MS (glycerol/TFA matrix) gave m/e = 640.0358 (MH^+, 20%, $C_{20}H_{26}N_5O_9S_5$; Calcd.

TABLE 3

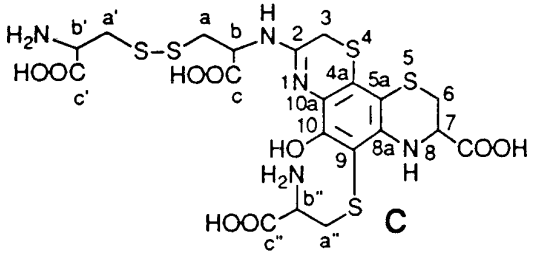

Assignment	^{1}H (J in Hz)	^{13}C	HMQC (^{13}C)	HMBC (^{13}C)
b	4.99 (dd, 8.5, 4.5, 1H)	56.04	56.04	171.42 (c), 154.04 (2), 37.05 (a)
7	4.58 (dd, 4.5, 3.5, 1H)	53.00	53.00	174.34 (c‴), 140.30 (8a)
b′	4.28 (dd, 8.0, 4.5, 1H)	51.68	51.68	170.63 (c′), 36.66 (a′)
b″	3.95 (dd, 6.0, 5.0, 1H)	52.47	52.47	170.35 (c″), 33.93 (a″)
3	3.83 (d, 15.0, 1H)	27.19	27.19	154.04 (2), 124.65 (4a)
3	3.79 (d, 15.0, 1H)	27.19	27.19	154.04 (2), 124.65 (4a)
a	3.48 (dd, 14.5, 4.5, 1H)	37.05	37.05	171.42 (c)
a′	3.34 (dd, 15.0, 4.5, 1H)	36.66	36.66	170.63 (c′)
a	3.20 (dd, 14.5, 8.5, 1H)	37.05	37.05	171.42 (c), 56.04 (b)
6	3.19 (dd, 13.0, 4.5, 1H)	25.52	25.52	103.55 (5a), 53.00 (7)
a″	3.18 (dd, 14.5, 6.0, 1H)	33.93	33.93	170.35 (c″), 100.75 (9), 52.47 (b″)
a′	3.13 (dd, 15.0, 8.0, 1H)	36.66	36.66	170.63 (c′), 51.68 (b′)
a″	3.11 (dd, 14.5, 5.0, 1H)	33.93	33.93	170.35 (c″), 100.75 (9)
6	3.02 (dd, 13.0, 3.5, 1H)	25.52	25.52	174.34 (c‴), 103.55 (5a), 53.00 (7)
8a		140.30		
10a		113.05		
2		154.04		
4a		124.65		
9		100.75		
10		146.81		
5a		103.55		
c		171.42		
c′		170.63		
c″		170.35		
c‴		174.34		

m/e = 640.0334). ^{1}H NMR (300 MHz, Me_2 SO-d_6) gave δ 6.44 (bs, 1H, N(8)-H), 5.08 (dd, J = 7.8, 5.1 Hz, 1H, C(b)-H), 4.47 (dd, J = 4.2, 3.6 Hz, 1H, C(7)-H), 4.13 (dd, J = 7.5, 4.8 Hz, 1H, C(b′)-H), 3.90 (dd, J = 9.0, 3.6 Hz, 1H, C(b″)-H), 3.47 (d, J = 14.7 Hz, 1H, C(3)-H), 3.40 (d, J = 14.7 Hz, 1H, C(3)-H), 3.34 (dd, J = 14.1, 5.1 Hz, 1H, C(a)-H), 3.31 (dd, J = 14.7, 4.8 Hz, 1H, C(a′)-H), 3.24 (dd, J = 14.1, 3.6 Hz, 1H, C(a″)-H), 3.22 (dd, J = 12.6, 4.2 Hz, 1H, C(6)-H), 3.15 (dd, J = 14.1, 7.8 Hz, 1H, C(a)-H), 3.14 (dd, J = 14.7, 7.5 Hz, 1H, C(a′)-H), 3.10 (dd, J = 12.6, 3.6 Hz, 1H, C(6)-H), and 3.01 (dd, J = 14.1, 9.0 Hz, 1H, C(a″)-H). The ^{1}H (500 MHz), ^{13}C (125 MHz), HMQC, and HMBC NMR spectra (D_2O), the proposed structure for **C,** and ^{1}H–^{13}C long-range connectivity assignments based on the HMBC results are presented in Table 3.

TABLE 4

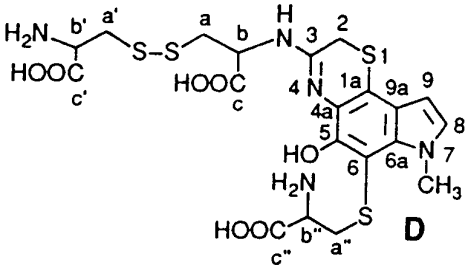

Assignment	^{1}H (J in Hz)	^{13}C	HMQC (^{13}C)	HMBC (^{13}C)
8	7.09 (d, 3.0, 1H)	130.43	130.43	131.71 (6a), 119.85 (9a), 98.89 (9), 37.08 (N(7)-CH_3)
9	6.19 (d, 3.0, 1H)	98.89	98.89	131.71 (6a), 130.43 (8), 119.85 (9a)
b	5.08 (dd, 8.0, 5.0, 1H)	53.47	53.47	172.13 (c), 150.99 (3), 39.00 (a)
b′	4.14 (dd, 7.0, 5.0, 1H)	51.37	51.37	169.57 (c′), 37.95 (a′)
7-CH_3	4.08 (s, 3H)	37.08	37.08	131.71 (6a), 130.43 (8)
b″	3.98 (t, 6.0, 1H)	52.16	52.16	169.46 (c″), 36.68 (a″)
2	3.52 (s, 2H)	24.14	24.14	150.99 (3), 112.61 (1a)
a	3.35 (dd, 13.5, 5.0, 1H)	39.00	39.00	172.13 (c)
a′	3.30 (dd, 14.5, 5.0, 1H)	37.95	37.95	169.57 (c′)
a″	3.22 (d, 6.0, 2H)	36.68	36.68	169.46 (c″), 95.97 (6), 52.16 (b″)
a	3.18 (dd, 13.5, 8.0, 1H)	39.00	39.00	172.13 (c), 53.47 (b)
a′	3.15 (dd, 14.5, 7.0, 1H)	37.95	37.95	169.57 (c′), 51.37 (b′)
9a		119.85		
1a		112.61		
3		150.99		
4a		125.46		
5		148.91		
6		95.97		
6a		131.71		
c		172.13		
c′		169.57		
c″		169.46		

N-[*6*-[(*2-Amino-2-carboxyethyl*)*thio*]-*2,7-dihydro-5-hydroxy-7-methylpyrrolo*[*2,3-h*]-*1,4-benzothiazin-3-yl*]-L-*cystine* (**D**)

Compound **D** was a pale yellow solid that, when dissolved in the HPLC mobile phase (pH 2.15), exhibited uv bands at λ_{max} = 338, 288, 264, and 220 nm. FAB-MS (glycerol/TFA matrix) gave m/e = 576.0684 (MH^+, 100%, $C_{20}H_{26}N_5O_7S_4$; Calcd. m/e = 576.0715). The proposed structure of **D,** its ^{1}H (500 MHz), ^{13}C (125 MHz), HMQC, and HMBC NMR spectra (Me_2SO-d_6) and long range ^{1}H–^{13}C connectivity assignments based on HMBC data are presented below in Table 4.

Cleavage of Disulfide Linkages of **C** *and* **D**

A stirred solution of **C** (10 mg) or **D** (9 mg) in 30 ml of deionized water was bubbled continuously with N_2 and the pH adjusted to 5.0 with 0.1 M aqueous KOH. TCEP·HCl (9 mg) was then added and the resulting stirred solution was again

adjusted to pH 5.0 with KOH. After 5 min, the entire solution was introduced onto the preparative HPLC column via one of the pumps. Using HPLC method IV, **E** (formed by TCEP reduction of **C**) and **F** (formed by TCEP reduction of **D**) eluted at 63 and 73 min, respectively. The eluent containing **E** or **F** was collected and freeze–dried. The resulting solid was dissolved in a minimum volume of deionized water and purified at least one time using HPLC method IV.

7-[(1-Carboxy-2-mercaptoethyl)amino]-10-[(2-amino-2-carboxyethyl)thio]-1,2,3,6-tetrahydro-9-hydroxy-benzo[1,2-b: 4,3-b′]bis[1,4]thiazine-2-carboxylic Acid (**E**)

Compound **E** was a yellow solid that, when dissolved in the HPLC mobile phase (pH 2.15), exhibited uv bands at λ_{max} = 374, 298 (sh), 260, and 228 nm. FAB-MS (dithiothreitol/dithioerythritol matrix) gave *m/e* = 521.0303 (MH^+, 6%, $C_{17}H_{21}N_4O_7S_4$; Calcd. *m/e* = 521.0293). ^{1}H NMR (300 MHz, Me_2 SO-d_6) gave δ 7.67 (bs, 1H, N(d)-H), 6.40 (bs, 1H, N(1)-H), 5.13–5.06 (m, 1H, C(b)-H), 4.46 (dd, J = 4.2, 3.6 Hz, 1H, C(2)-H), 3.91 (dd, J = 8.7, 3.6 Hz, 1H, C(b″)-H), 3.47 (d, J = 14.7 Hz, 1H, C(6)-H), 3.40 (d, J = 14.7 Hz, 1H, C(6)-H), 3.22 (dd, J = 14.1, 3.6 Hz, 1H, C(a″)-H), 3.21 (dd, J = 12.9, 4.2 Hz, 1H, C(3)-H), 3.11 (dd, J = 12.9, 3.6 Hz, 1H, C(3)-H), 3.00 (dd, J = 14.1, 8.7 Hz, 1H, C(a″)-H), 2.99 (dd, J = 13.8, 5.1 Hz, 1H, C(a)-H), 2.88 (dd, J = 13.8, 6.0 Hz, 1H, C(a)-H).

*N-[6-[(2-Amino-2-carboxyethyl)thio]-2,7-dihdydro-5-hydroxy-7-methylpyrrolo[2,3-h]-1,4-benzothiazin-3-yl]-*L*-cysteine* (**F**)

Compound **F** was a pale yellow solid that, when dissolved in the HPLC mobile phase (pH 2.15), exhibited uv bands at λ_{max} = 338, 288, 264, and 220 nm. FAB-MS (dithiothreitol/dithioerythritol matrix) gave *m/e* = 457.0675 (MH^+, 17%, $C_{17}H_{21}N_4O_5S_3$; Calcd. *m/e* = 457.0674). ^{1}H NMR (300 MHz, Me_2 SO-d_6) gave δ 7.94 (bs, 1H, N(d)-H), 7.11 (d, J = 3.0 Hz, 1H, C(8)-H), 6.21 (d, J = 3.0 Hz, 1H, C(9)-H), 5.15–5.07 (m, 1H, C(b)-H), 4.10 (s, 3H, CH_3), 4.04 (t, J = 6.3 Hz, 1H, C(b″)-H), 3.52 (s, 2H, C(2)-H_2), 3.23 (d, J = 6.3 Hz, 2H, C(a″)-H_2), 3.04 (dd, J = 13.8, 4.5 Hz, 1H, C(a)-H), 2.92 (dd, J = 13.8, 6.0 Hz, 1H, C(a)-H).

RESULTS

Cyclic Voltammetry

Cyclic voltammograms of DA, NE, and EPI dissolved in pH 7.4 phosphate buffer at a sweep rate (ν) of 100 mV s^{-1} are shown in Fig. 1. The reactions responsible for the various peaks observed in these voltammograms are readily understood with reference to Scheme 1 (*9–15*). Thus, peak I_a corresponds to the reversible oxidation (2*e*, $2H^+$) of the catecholamines to their respective *o*-quinones and peak I_c to the reverse reaction. Peak II_c corresponds to the reversible reduction of the aminochrome **2** to 5,6-dihydroxyindoline **1** and peak II_a to the reverse reaction. Thus, the reaction pathways for the oxidation of all the catecholamine neurotransmitters are fundamentally the same. However, the rates of intramolecular cyclization

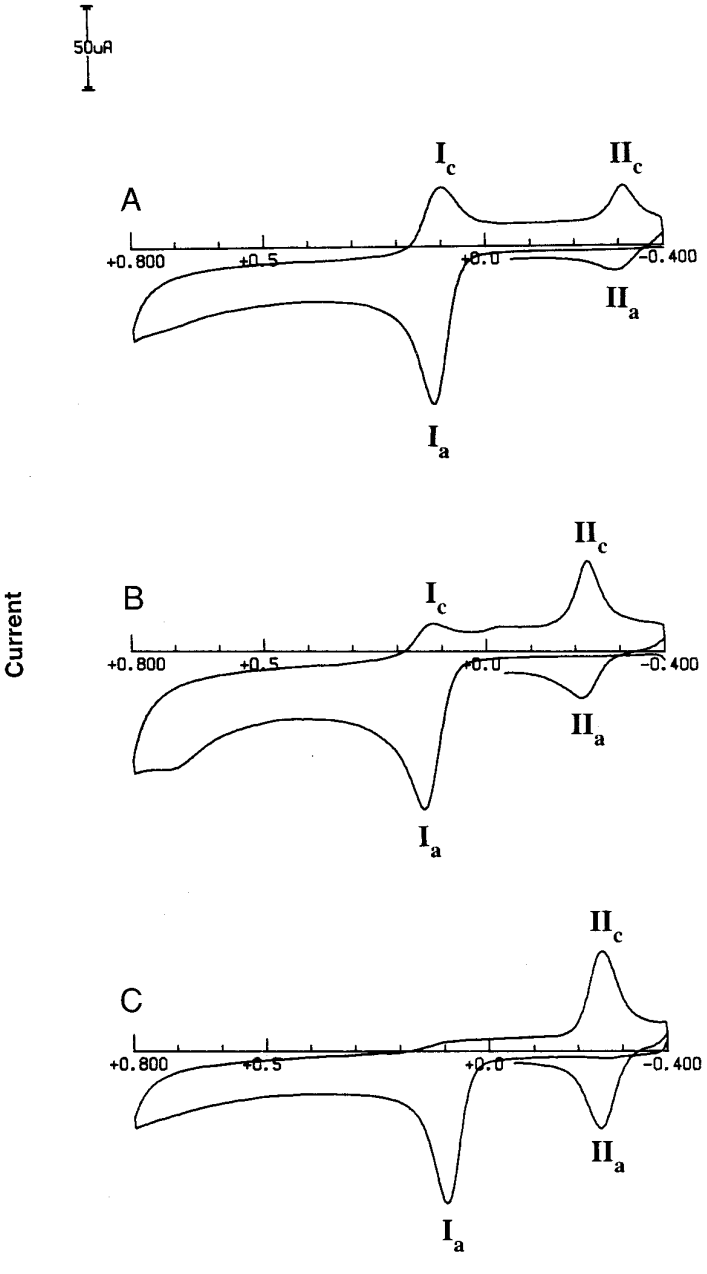

FIG. 1. Cyclic voltammograms at the PGE of 0.5 mM solutions of (A) DA, (B) NE, and (C) EPI in pH 7.4 phosphate buffer (μ = 1.0). Sweep rate: 100 mV s^{-1}.

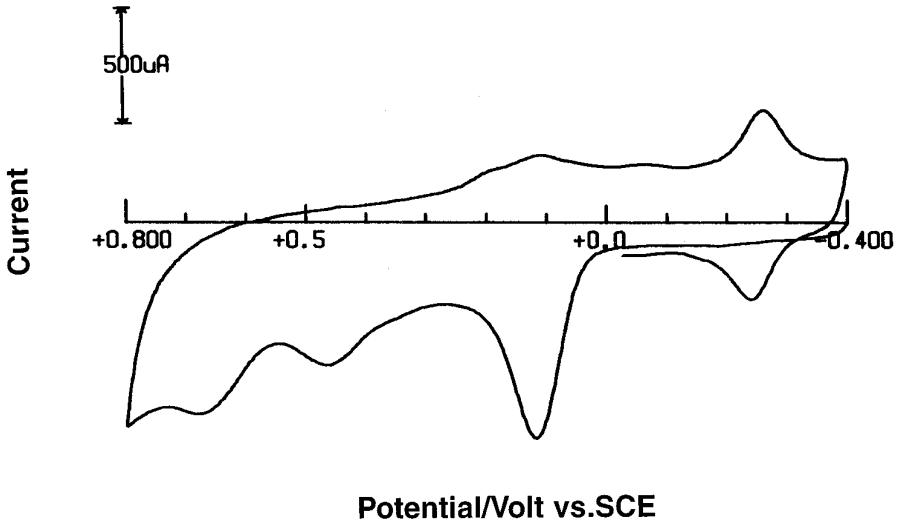

FIG. 2. Cyclic voltammogram at the PGE of 0.5 mM 5-*S*-CyS-EPI in pH 7.4 phosphate buffer (μ = 1.0). Sweep rate: 5 V s^{-1}.

of the *o*-quinones, formed upon oxidation of these compounds, and subsequent oxidation of the 5,6-dihydroxyindoline **1** to aminochrome **2** are appreciably different. This reaction sequence is most rapid for EPI-*o*-quinone (*12*) with the result that peak I_c cannot be observed in the cyclic voltammogram of EPI, whereas the peak II_c/peak II_a couple is very large (Fig. 1C). A comparison of the cyclic voltammograms of DA, NE, and EPI reveals that the rate of this reaction sequence decreases in the order EPI-*o*-quinone $\gg$ NE-*o*-quinone $>$ DA-*o*-quinone.

The major initial products of nucleophilic addition of CySH to the *o*-quinones formed by oxidation of DA, NE, and EPI are the 5-*S*-cysteinyl conjugates of these neurotransmitters (*1–6*). A cyclic voltammogram (ν = 5 V s^{-1}) of 5-*S*-CyS-EPI at pH 7.4 (Fig. 2) reveals that after scanning through its primary oxidation peak a reversible couple appears at $E^{\circ\prime} = -249$ mV after scan reversal. This couple is a prominent feature of cyclic voltammograms of 5-*S*-CyS-EPI at all sweep rates studied (500 mV s^{-1}-10 V s^{-1}). Cyclic voltammograms (ν = 5 V s^{-1}) of 2-*S*-CyS-EPI and 2,5-bis-*S*-CyS-EPI also exhibited similar reversible follow-up couples at $E^{\circ\prime} = -248$ and -246 mV, respectively. Under the same conditions the 5-*S*-, 2-*S*-, and 2,5-bis-*S*-cysteinyl conjugates of DA (*1*, *2*) and NE (*5*) do not give rise to these reversible follow-up couples in their cyclic voltammograms. The preceding observations indicate that the cysteinyl conjugates of EPI differ from those of DA and NE in that they can be not only oxidatively transformed into DHBTs (Scheme 2) but also that intramolecular cyclization of the β-hydroxy-(*N*-methyl)ethylamino side chain can occur to give aminochromes responsible for the reversible couples at $E^{\circ\prime} \approx -248$ mV observed in their cyclic voltammograms.